九州大学学術情報リポジトリ
Kyushu University Institutional Repository

Pulmonary arterial input impedance reflects the mechanical properties of pulmonary arterial remodeling in rats with pulmonary hypertension

西川, 拓也

https://hdl.handle.net/2324/2236135

出版情報：Kyushu University, 2018, 博士（医学）, 課程博士
バージョン：
権利関係：

KYUSHU UNIVERSITY

Life Sciences 212 (2018) 225–232

Contents lists available at ScienceDirect

Life Sciences

journal homepage: www.elsevier.com/locate/lifescie

Pulmonary arterial input impedance reflects the mechanical properties of pulmonary arterial remodeling in rats with pulmonary hypertension

Takuya Nishikawa[a,b,*], Keita Saku[c], Takuya Kishi[c], Takeshi Tohyama[a], Kohtaro Abe[a], Yasuhiro Oga[a], Takahiro Arimura[a], Takafumi Sakamoto[a], Keimei Yoshida[a], Kenji Sunagawa[d], Hiroyuki Tsutsui[a]

[a] Department of Cardiovascular Medicine, Kyushu University Graduate School of Medical Sciences, Fukuoka, Japan
[b] Department of Cardiovascular Dynamics, National Cerebral and Cardiovascular Center, Suita, Japan
[c] Department of Advanced Risk Stratification for Cardiovascular Diseases, Center for Disruptive Cardiovascular Medicine, Kyushu University, Fukuoka, Japan
[d] Department of Therapeutic Regulation of Cardiovascular Homeostasis, Center for Disruptive Cardiovascular Medicine, Kyushu University, Fukuoka, Japan

ARTICLE INFO

Keywords:
Pulmonary hypertension
Input impedance
Pulmonary arterial compliance
Hemodynamics

ABSTRACT

Aims: Although pulmonary arterial remolding in pulmonary hypertension (PH) changes the mechanical properties of the pulmonary artery, most clinical studies have focused on static mechanical properties (resistance), and dynamic mechanical properties (compliance) have not attracted much attention. As arterial compliance plays a significant role in determining afterload of the right ventricle, we evaluated how PH changes the dynamic mechanical properties of the pulmonary artery using high-resolution, wideband input impedance (Z_{PA}). We then examined how changes in Z_{PA} account for arterial remodeling. Clarification of the relationship between arterial remodeling and Z_{PA} could help evaluate arterial remodeling according to hemodynamics.

Main methods: PH was induced in Sprague–Dawley rats with an injection of Sugen5416 (20 mg/kg) and 3-week exposure to hypoxia (10% oxygen) (SuHx). Z_{PA} was evaluated from pulmonary artery pressure and flow under irregular pacing. Pulmonary histology was examined at baseline and 1, 3, and 8 weeks ($n = 7$, each) after Sugen5416 injection.

Key findings: SuHx progressively increased pulmonary arterial pressure. Z_{PA} findings indicated that SuHx progressively increased resistance (baseline: 9.3 ± 3.6, SuHx1W: 20.7 ± 7.9, SuHx3W: 48.8 ± 6.9, SuHx8W: 62.9 ± 17.8 mm Hg/mL/s, $p < 0.01$) and decreased compliance (baseline: 11.9 ± 2.1, SuHx1W: 5.3 ± 1.7, SuHx3W: 2.1 ± 0.7, SuHx8W: 1.9 ± 0.6 × 10^{-3} mL/mm Hg, $p < 0.01$). The time constant did not significantly change. The progressive reduction in compliance was closely associated with wall thickening of small pulmonary arteries.

Significance: The finding that changes in resistance were reciprocally associated with those in compliance indicates that resistant and compliant vessels are anatomically inseparable. The analysis of Z_{PA} might help evaluate arterial remodeling in PH according to hemodynamics.

1. Introduction

Pulmonary hypertension (PH) is a multifactorial complex pulmonary vascular disorder. Pulmonary arterial remodeling and functional vasoconstriction have been shown to increase pulmonary resistance and artery pressure and consequently cause life–threatening right ventricular (RV) failure and death [1,2]. Such structural and functional alterations in pulmonary vasculature change its mechanical properties [3]. Therefore, detailed analyses of its mechanical properties would enable the identification of the severity of arterial remodeling. However, most clinical studies have focused on static mechanical properties (resistance) without assessing dynamic mechanical properties (compliance).

In the systemic arterial system, aortic input impedance, which is the

Abbreviations: PH, pulmonary hypertension; RV, right ventricular; 3-WK, 3-element windkessel; Z_{PA}, pulmonary arterial input impedance; SV, stroke volume; PP, pulse pressure; SuHx, Sugen/hypoxia; RVH, right ventricular hypertrophy; ODs, outer diameters; WT50, arteries with ODs < 50 μm; WT100, arteries with ODs 50–100 μm; P_{PA}, Pulmonary artery pressure; F_{PA}, Pulmonary artery flow

* Corresponding author at: Department of Cardiovascular Medicine, Kyushu University Graduate School of Medical Sciences, Kyushu University, 3-1-1 Maidashi, Higashi-ku, Fukuoka 812-8582, Japan.
E-mail address: nisikawa@cardiol.med.kyushu-u.ac.jp (T. Nishikawa).

https://doi.org/10.1016/j.lfs.2018.10.005
Received 3 August 2018; Received in revised form 4 October 2018; Accepted 5 October 2018
Available online 06 October 2018
0024-3205/ © 2018 The Authors. Published by Elsevier Inc. This is an open access article under the CC BY license (http://creativecommons.org/licenses/BY/4.0/).

ratio of arterial pressure to flow in the frequency domain, has been used to assess the dynamic mechanical properties of arterial vasculature [4,5]. Westerhof et al. [6] approximated systemic arterial input impedance using a 3-element windkessel (3-WK) (resistance, compliance, and characteristic impedance) model.

As the basic structure of the pulmonary arterial system resembles that of the systemic arterial system, many investigators have adopted the 3-WK model to approximate pulmonary arterial input impedance (Z_{PA}) [7]. In the evaluation of PH, pulmonary arterial resistance reflects PH severity and predicts long-term outcome [8]. In contrast, compliance has been rarely assessed because its measurement is technically difficult and its relationship with pathophysiology remains unestablished. Rosen et al. proposed a practical method to estimate compliance according to the ratio of stroke volume (SV) to pulse pressure (PP) [9]. However, SV/PP does not necessarily provide an accurate estimate of compliance, as changes in the pulmonary artery and/or RV condition, such as characteristic impedance and contractility, could affect PP [10]. Characteristic impedance is the ratio of magnitude of pressure and flow waves in an infinite transmission line. It is often measured from the input impedance using the average values of high frequency moduli [11,12]. However, it is controversial whether PH alters characteristic impedance [13–16], because the complexity of wave reflections in PH prevents precise assessment. The time constant of impedance manifests as a corner frequency. However, in the physiological condition, the corner frequency is lower than the heart rate frequency. Thus, the estimation of the time constant from Z_{PA} under a regular heart rate is imprecise. We believe that such technical difficulties make the clinical applications of pulmonary impedance impractical.

As we focused on dynamic pulmonary vascular properties in this study, we used a Sugen/Hypoxia model of PH (SuHx) considering that its histological phenotype of pulmonary vascular remodeling is similar to that of PH in humans [17]. In the PH model rats, we assessed Z_{PA} by using a random perturbation method [5]. This makes the impedance estimation wideband and high-resolution and allows precise estimation of the time constant below the heart rate frequency. Furthermore, to avoid inaccuracy resulting from complex wave reflections, we estimated characteristic impedance from the instantaneous pressure–flow relationship in the time domain before the reflected waves could influence the relation. Using the determined characteristic impedance, we derived the remaining two parameters of the 3-WK model from the Z_{PA} and examined their relationships with pulmonary arterial remodeling.

2. Material and methods

2.1. Animal preparations and experimental protocols

The Committee on Ethics of Animal Experiments, Kyushu University Graduate School of Medical Sciences approved the experiments and animal care. The experiments were performed in strict accordance with the Guide for the Care and Use of Laboratory Animals published by the US National Institutes of Health.

The study included male Sprague–Dawley rats weighing 190–210 g. The rats were subcutaneously injected with Sugen5416 (20 mg/kg; Cayman Chemical, Ann Arbor, MI) and were exposed to hypoxia (10% O_2) for 3 weeks. They were returned to normoxia (21% O_2) thereafter. As shown in Fig. 1A, we assessed hemodynamics and histology at baseline (before the Sugen5416 injection) and 1, 3, and 8 weeks after the Sugen5416 injection ($n = 7$ in each period).

2.2. Preparation

All rats were anesthetized with an intraperitoneal injection (2 mL/kg) of a mixture of α-chloralose (40 mg/mL) and urethane (250 mg/mL) and were mechanically ventilated with oxygen-enriched gas. A heating pad was used to maintain their body temperature at approximately 38 °C.

Left thoracotomy was performed, and pulmonary arterial pressure was measured with a catheter-tipped micromanometer (SPR-320; Millar Instruments, Houston, TX) inserted into the pulmonary trunk. Additionally, an ultrasonic flow probe (model 2PS; Transonic, Ithaca, NY) was placed at the pulmonary trunk to measure pulmonary artery flow. Moreover, a pair of stainless steel wire electrodes (Bioflex wire AS633; Cooner Wire, Chatsworth, CA) was attached to the left ventricle to pace the heart according to a computer-generated random binary sequence (2–10 Hz) (Fig. 1B).

2.3. Data acquisition

All hemodynamic time series were digitized at 1000 Hz (Power Lab 16/35; ADInstruments, NSW, Australia) and stored in a dedicated laboratory computer system. We corrected the time delay of the flow measuring system (Supplement 1) to align pulmonary arterial pressure and flow.

2.4. Pulmonary arterial input impedance

We estimated high-resolution wideband pulmonary arterial input impedance from the time series of pulmonary arterial pressure and flow for 90.112 s under irregular cardiac pacing. The time series were segmented into 10 sets of 50% overlapping bins of 16,384 points each. After detrending, pulmonary arterial pressure and flow were windowed with a 4-term Blackman–Harris window and were then Fourier transformed. The power spectra of pulmonary arterial pressure [$|P_{PA}(f)|^2$] and flow [$|F_{PA}(f)|^2$] and their crosspower spectra [$P_{PA}(f)\cdot F_{PA}{}^*(f)$] were calculated in each bin and then ensembled over the 10 segments. Finally, we estimated the impedance [$Z_{PA}(f)$] in the frequency range between 0.1 Hz and 100 Hz with a resolution of 0.061 Hz by the following equation.

$$Z_{PA}(f) = \frac{P_{PA}(f)\cdot F_{PA}{}^*(f)}{|F_{PA}(f)|^2}$$

We also estimated the magnitude squared coherence [Coh(f)] which indicates the linear dependence of pulmonary arterial pressure and flow using the following equation:

$$Coh(f) = \frac{|P_{PA}(f)\cdot F_{PA}{}^*(f)|^2}{|F_{PA}(f)|^2\cdot|P_{PA}(f)|^2}$$

where Coh(f) varies between 0 and 1.

2.5. Estimation of each element in the 3-WK model

We estimated each element in the 3-WK model (Fig. 2A). In most previous studies, characteristic impedance was determined by averaging the impedance moduli in the high-frequency range [16]. However, unlike aortic input impedance, high-frequency impedance varies considerably particularly in PH, because of complex reflections in the pulmonary artery. These complex reflections make the estimation of characteristic impedance in the frequency domain imprecise. To avoid this limitation, we estimated characteristic impedance in the time domain [18]. Briefly, characteristic impedance is defined by the ratio of forward pressure to forward flow. As the reflected waves do not contaminate the upstroke phase of pulmonary arterial pressure and flow, consideration of the ratio of pulmonary arterial pressure to flow in the beginning of ejection should yield characteristic impedance. We assessed characteristic impedance by calculating the linear slope of the instantaneous pressure–flow relationship in the first 10 ms of ejection and obtaining the average value over 30 beats (Fig. 2B).

After determining characteristic impedance, we used its value, fit the 3-WK model to the measured high-resolution, wideband impedance at a frequency of up to 10 Hz, and determined resistance and compliance with the non-linear least-square method using the trust region

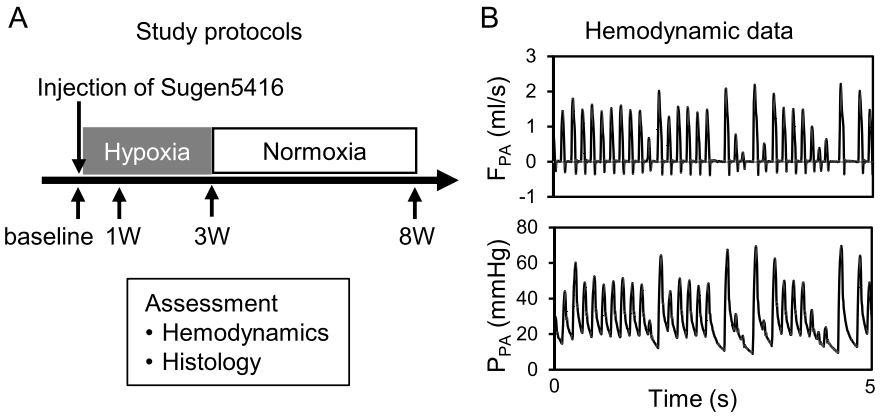

Fig. 1. Experimental protocol (A). Representative time series of pulmonary artery flow (F_{PA}) and pulmonary artery pressure (P_{PA}) under irregular cardiac pacing (B).

reflective algorithm [19] (Matlab R2017b, MathWorks, Natick, MA; time–frequency method) (Fig. 2C). The time constant was obtained by multiplying resistance with compliance.

2.6. Right ventricular hypertrophy

We excised the heart, dissected the right ventricle from the left ventricle and the septum, and weighed them separately. Right ventricular hypertrophy (RVH) was indexed by the weight ratio of the right ventricle to the left ventricle plus the septum [20].

2.7. Histological analysis

After hemodynamic measurements, we injected barium–gelatin at 70 °C into the pulmonary arteries while keeping the pressure at the individual mean pulmonary arterial pressure as previously reported [21]. All sections were stained with Verhoeff–van Gieson for histological analysis. We determined the external elastic lamina and vascular lumen. We then defined the circularity of the pulmonary artery by dividing the measured total vascular area (the area circumscribed by the external elastic lamina) by the maximum area calculated from the perimeter length. Unity circularity indicates that the arterial cross section is a perfect circle. We examined barium-filled arteries with outer diameters (ODs) < 100 μm and circularity > 0.6. We calculated wall thickness using the following equation:

$$\text{Wall thickness} = \frac{\text{Total vascular area} - \text{Vascular lumen area}}{\text{Total vasucular area}}$$

2.8. Statistical analysis

Data are presented as mean ± standard deviation. We used ANOVA with post-hoc Tukey-Kramer's test for multiple comparisons among the experimental groups. Additionally, we used ANCOVA for comparisons of the slopes of regression lines between wall thickness and hemodynamic parameters. All statistical analyses were performed using JMP version 11 (SAS Institute, Cary, NC). Differences were considered significant at $p < 0.05$.

3. Results

3.1. Changes in the mean pulmonary arterial pressure, flow, and RVH

Body weight increased with time (baseline: 205 ± 5.9 g, SuHx1W: 217 ± 5.7 g, SuHx3W: 263 ± 7.3 g, SuHx8W: 365 ± 53.8 g, $p < 0.01$). As shown in Fig. 3, the mean pulmonary arterial pressure progressively increased and tripled 8 weeks after the Sugen5416 injection (baseline: 19.5 ± 1.9 mm Hg, SuHx1W: 26.1 ± 3.1 mm Hg, SuHx3W: 45.6 ± 5.5 mm Hg, SuHx8W: 63.9 ± 13.4 mm Hg, $p < 0.01$; Fig. 3A). RVH was consistent with the progression of PH (Fig. 3C). However, irrespective of the increase in pulmonary arterial pressure, pulmonary arterial flow remained unchanged (Fig. 3B).

3.2. Alteration of pulmonary arterial input impedance in SuHx rats

Fig. 4 shows the high-resolution, wideband pulmonary arterial input impedance (Z_{PA}) plotted on the logarithmic scale in moduli and

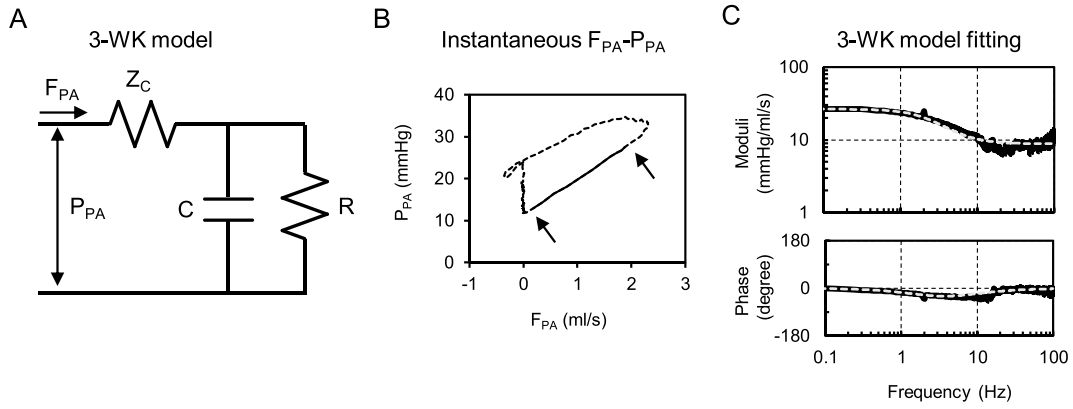

Fig. 2. The 3-element windkessel (3-WK) model (A). The model consists of characteristic impedance (Z_C), resistance (R), and compliance (C). Instantaneous relationship of pulmonary artery flow (F_{PA}) and pressure (P_{PA}) (B). The upstroke limb (the solid line between two arrows) of the instantaneous arterial pressure (P_{PA}) and flow (F_{PA}) relation (dashed line) is virtually liner. Its slope represents Z_C. Comparison of the measured pulmonary arterial input impedance (Z_{PA}, solid line) and the impedance estimated from the 3-WK model (dashed line). Top and bottom panels show the impedance moduli and phase, respectively.

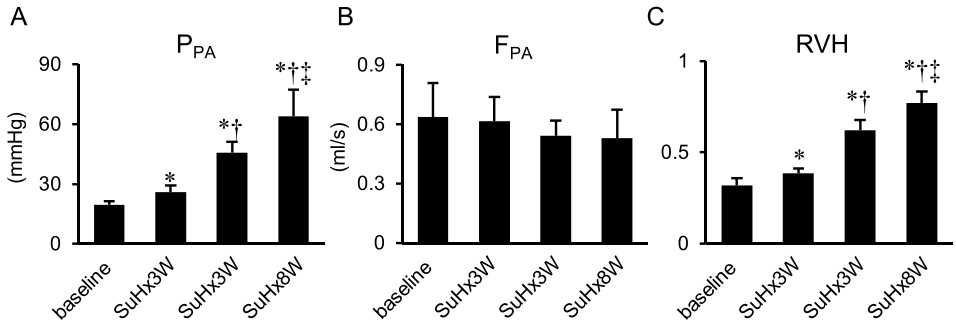

Fig. 3. The time course of pulmonary arterial pressure (P_{PA}) (A), pulmonary arterial flow (F_{PA}) (B), and right ventricular hypertrophy (RVH) (C) in Sugen/hypoxia (SuHx) rats. P_{PA} and RVH increase with time. F_{PA} remains unchanged. *$p < 0.05$ vs. baseline, †$p < 0.05$ vs. SuHx1W, ‡$p < 0.05$ vs. SuHx3W.

frequency at baseline and 1, 3, and 8 weeks after the Sugen5416 injection. In general, progression of PH shifted the impedance moduli upward. At baseline, moduli below 1 Hz were relatively constant with little shift in phase, indicating the resistive property of Z_{PA}. In the frequency range between 1 and 20 Hz, the moduli decreased with frequency, with significant delays in phase, indicating the capacitive property of Z_{PA}. Above 20 Hz, the moduli were relatively stable at baseline and were highly variable with the progression of PH. These moduli instabilities in the high-frequency range make frequency domain estimation of characteristic impedance imprecise and thereby impractical.

3.3. Dynamic properties

Fig. 5 shows the 3-WK model parameters obtained from high-resolution, wideband pulmonary arterial input impedance. SuHx progressively increased resistance (baseline: 9.3 ± 3.6 mm Hg/mL/s, SuHx1W: 20.7 ± 7.9 mm Hg/mL/s, SuHx3W: 58.8 ± 6.9 mm Hg/mL/s, SuHx8W: 62.9 ± 17.8 mm Hg/mL/s, $p < 0.01$; Fig. 5A) and decreased compliance (stiffening the vessels) (baseline: 11.9 ± 2.1 × 10^{-3} mL/mm Hg, SuHx1W: 5.3 ± 1.7 × 10^{-3} mL/mm Hg, SuHx3W: 2.1 ± 0.7 × 10^{-3} mL/mm Hg, SuHx8W: 1.9 ± 0.6 × 10^{-3} mL/mm Hg, $p < 0.01$; Fig. 5B). Characteristic impedance and the time constant remained unaltered regardless of the progression of PH (Fig. 5C and D, respectively).

3.4. Histological analysis

The progression of pulmonary arterial remodeling and the corresponding wall thickening in arteries with ODs < 50 μm (WT50) and 50–100 μm (WT100) across the assessment points are shown in Fig. 6. The wall thickness was found to have tripled in WT50 and doubled in WT100, indicating more severe vascular remodeling in smaller arteries. The markedly increased wall thickness in the smaller arteries indicated that the lumen area predominantly decreased in the smaller arteries. The reduction in the lumen area of the smaller arteries would have had a major impact on pulmonary arterial resistance.

Fig. 7 shows the relationships of resistance and compliance with wall thickness. The slope of the relationship between resistance and wall thickness was steeper in the smaller arteries (Fig. 7A) than in the larger arteries (Fig. 7B) (243.5 vs. 156 mL/s/mm Hg, $p < 0.01$), indicating that wall thickening (lumen area loss) of smaller arteries plays an important role in determining pulmonary artery resistance. Additionally, the slope of the relationship between compliance and wall thickness was steeper in the smaller arteries (Fig. 7C) than in the larger arteries (Fig. 7D) (−54.2 vs. −39.2 × 10^3 mm Hg/mL, $p < 0.01$), indicating that wall thickening of smaller arteries plays an important role in determining compliance.

4. Discussion

In a rat model of SuHx PH, we investigated how PH affects

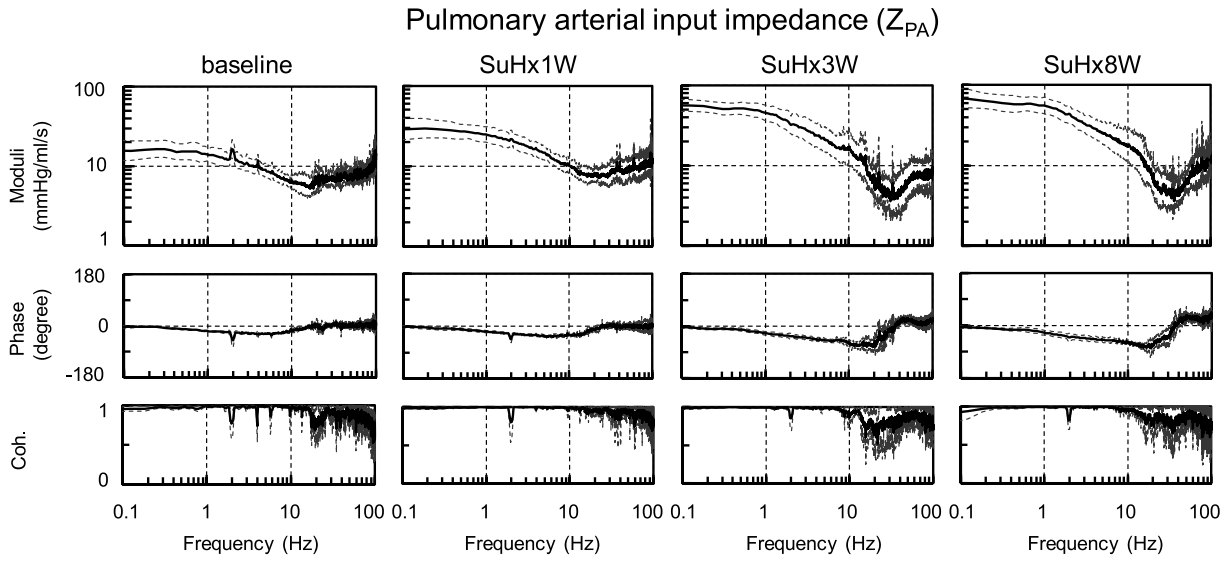

Fig. 4. Changes in pulmonary arterial input impedance (Z_{PA}) in Sugen/hypoxia (SuHx) rats. Impedance moduli phase (degree), and coherence are shown. The moduli at a frequency < 10 Hz increase with the progression of pulmonary hypertension, while the phases remain relatively unaltered. The solid and dashed lines represent mean and mean ± standard deviation, respectively. Coh, magnitude squared coherence.

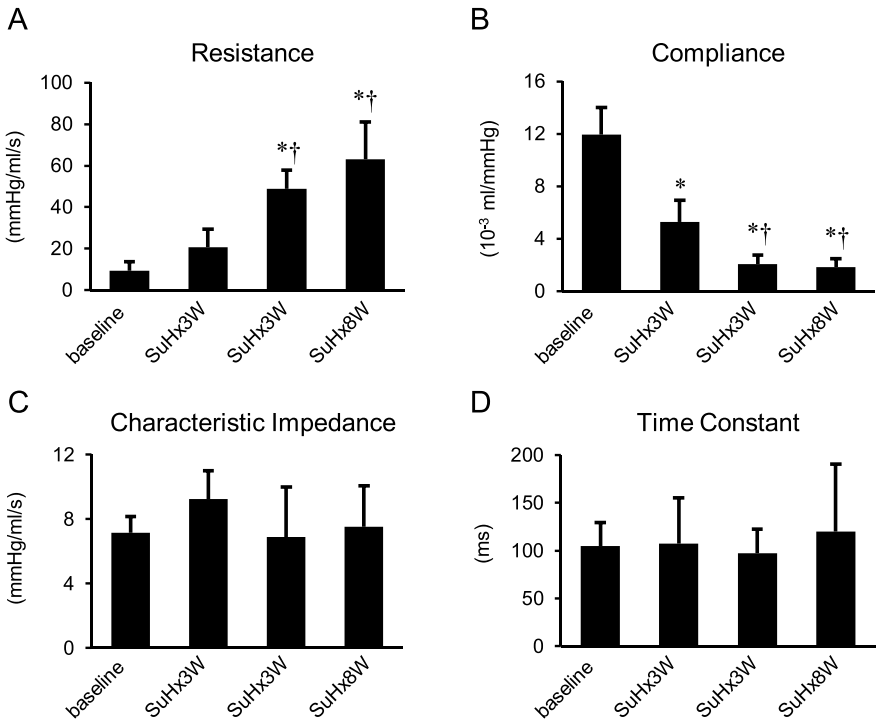

Fig. 5. Changes in resistance (A), compliance (B), characteristic impedance (C), and the time constant (D) in Sugen/hypoxia (SuHx) rats. With the progression of pulmonary hypertension, resistance increases, whereas compliance decreases. Characteristic impedance and time constant remain unaltered. *$p < 0.05$ vs. baseline, †$p < 0.05$ vs. SuHx1W.

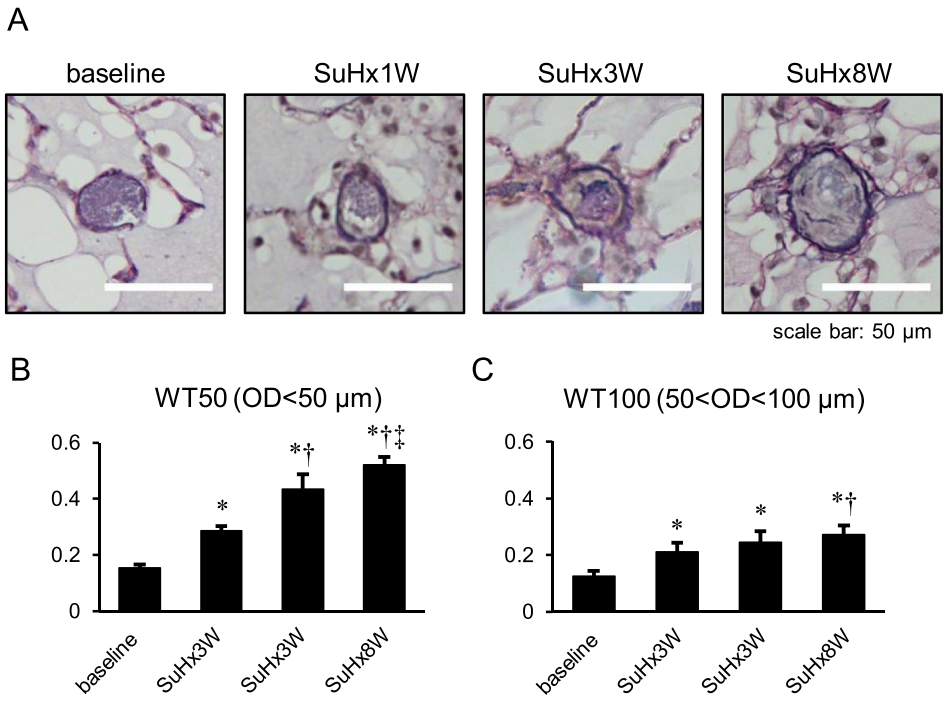

Fig. 6. Histological analysis of the pulmonary arteries stained with Verhoeff–van Gieson. The top panels (A) show the progression of pulmonary arterial remodeling. The bottom panels show the corresponding wall thickening in arteries with outer diameters < 50 μm (WT50) (B) and 50–100 μm (WT100) (C). Sugen/hypoxia (SuHx)-induced pulmonary hypertension increased both WT50 and WT100. *$p < 0.05$ vs. baseline, †$p < 0.05$ vs. SuHx1W. SuHx, Sugen/hypoxia.

pulmonary vascular mechanics by analyzing high-resolution, wideband pulmonary impedance (Z_{PA}). We found that the moduli of Z_{PA} shifted upward in SuHx PH model rats, and the degree of the upward shift in Z_{PA} was consistent with the progression of PH. Additionally, the upward shift in Z_{PA} accompanied increases in resistance and decreases in compliance. However, the time constant and characteristic impedance remained unchanged. Moreover, the histological study showed that the increases in resistance and decreases in compliance were closely associated with increases in the wall thickness of arteries with ODs < 50 μm.

4.1. Alteration of Z_{PA} in PH model rats

As the structural alterations of the pulmonary artery in PH are tightly associated with its mechanical properties [3], experiments using an animal model in which pulmonary vascular remodeling resembles that in human PH are essential for understanding its pathophysiology. Therefore, we used SuHx PH model in this study, which closely resembles with human PH [17].

In this study, we noted moduli instability and variability in the high-frequency range, and thus, the derivation of characteristic impedance by averaging the moduli was impractical. Therefore, we developed a

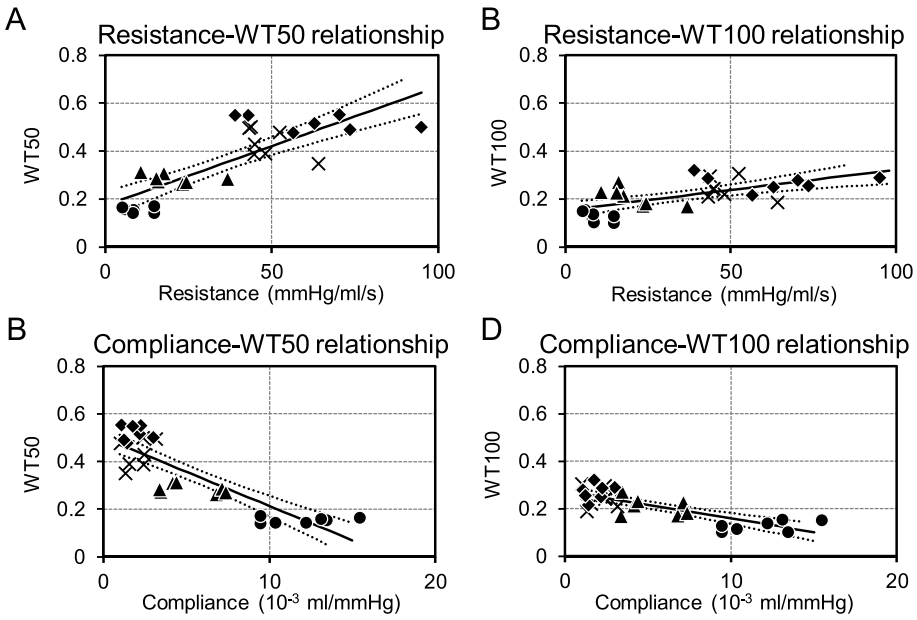

Fig. 7. The relationship between arterial wall thickness histologically determined and the mechanical properties of the pulmonary arteries. The top two panels show the relationship between resistance and WT50 (A) or WT100 (B). The bottom two panels show the relationship between compliance and WT50 (C) or WT100 (D). Changes in both resistance and compliance are more closely associated with WT50 than with WT100. The circles, triangles, squares, and crosses represent baseline, SuHx1W, SuHx3W, and SuHx8W, respectively. The solid and dotted lines represent regression lines and their 95% confidence intervals, respectively. WT50 and WT100 are wall thickening in arteries with outer diameter < 50 μm and 50–100 μm, respectively. SuHx, Sugen/hypoxia.

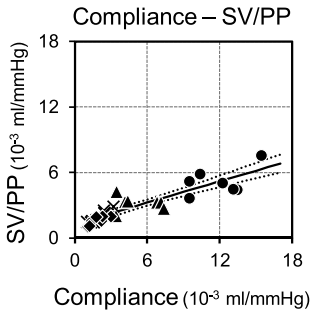

Fig. 8. The relationship between compliance estimated with the time-frequency method and with the ratio of stroke volume to pulse pressure (SV/PP). Although compliance values estimated with the time–frequency method and SV/PP show a positive correlation, the former is nearly twice as large as the latter. The circles, triangles, squares, and crosses represent baseline, SuHx1W, SuHx3W, and SuHx8W, respectively. The solid and dotted lines represent regression lines and their 95% confidence intervals. SuHx, Sugen/hypoxia.

new technique (the time–frequency method) to estimate the parameter values of the 3-WK model. Fig. 8 shows the relationship between compliance estimated with the time–frequency method and SV/PP. Although compliance correlated linearly with SV/PP, it was generally larger than SV/PP. As PP is the sum of the pressure generated by the volume in arterial compliance and that generated by flow and characteristic impedance, the measured PP would be higher than the PP generated by compliance alone. Therefore, we speculate that 3-WK model parameters are identified more precisely with the time–-frequency method than with SV/PP.

As shown in Fig. 5, with the progression of PH, resistance increased six times and compliance decreased to 1/6 at 8 weeks when compared to the values at baseline. Thus, the time constant remained unchanged irrespective of the progression of PH. In the early stage among SuHx PH model rats, decreases in compliance were more evident than increases in resistance. On the other hand, in the late stage, decreases in compliance were limited as arterial wall stiffness reached its maximum value. These results indicate that the assessment of compliance might contribute to the early detection of PH in clinical settings.

4.2. Relationship between changes in impedance and pulmonary vascular morphology

Previous clinical studies on PH, in which compliance was evaluated with SV/PP, reported that an increase in resistance was associated with a decrease in compliance, without a change in the time constant [22–24]. Our histological study indicated that changes in resistance and compliance are closely associated with the wall thickness of small arteries with ODs < 50 μm. Wall thickening in small arteries is possible to narrow the lumen area and increase resistance. As shown in the Supplemental Table 1, PH significantly reduced the lumen to wall ratio, indicating the narrowing of lumen area with the increased wall thickness in this study. Moreover, resistance is proportional to the inverse square of the lumen area according to the Hagen–Poiseuille law [25]. In this study, as WT50 indicates the lumen area normalized by the total vascular area, we can estimate how changes in WT50 affect resistance using the following equation:

$$\frac{R_{PH}}{R_{Baseline}} = \frac{(1 - WT50_{Baseline})^2}{(1 - WT50_{PH})^2}$$

where $R_{PH}/R_{Baseline}$, $WT50_{Baseline}$, and $WT50_{PH}$ are the ratio of resistance from baseline, WT50 at baseline, and WT50 at PH, respectively. The estimated resistance change associated with wall thickness was nearly three-fold higher than real values at SuHx8W. However, this does not fully explain the six-fold increase in resistance in PH. Nevertheless, it is well known that severe remodeling in established PH often occludes many small arteries [26,27]. Therefore, it is conceivable that the increased resistance of small arteries and the reduced number of small arteries might account for the six-fold increase in pulmonary arterial resistance. However, we cannot directly compare the number of small arteries among the progression phases of PH because the thinness of pulmonary arterial wall in the earlier phase of PH obscured the detection of arteries (Supplement 2).

The factors that change compliance in PH are not clear. As shown in Fig. 6B, wall thickness increased by three-fold in small arteries. If the material properties of the wall did not change, this thickening alone would explain the reduction in compliance to 1/3. However, in small arteries, thickening of the vascular wall narrows the lumen area, and thus, vascular wall stress reduces (Laplace law). This would at least partly explain the disproportional decrease in compliance in PH beyond simple wall thickening. Changes in material properties of the pulmonary arterial wall could affect Z_{PA}. Kobs et al. reported that PH

increased both collagen and elastin of pulmonary arteries and stiffened the pulmonary arteries [28]. Further investigations are needed to clarify the contribution of each component to changes in the pulmonary arterial mechanical properties. Furthermore, as discussed above, the number of small arteries would be less in PH. Moreover, it is well known that vascular material stiffens when intravascular pressure increases [29]. Thus, it is possible that a high pulmonary arterial pressure stiffened large arteries and reduced compliance. Nevertheless, it remains difficult to explain how changes in compliance are exactly reciprocal to changes in resistance. They are unlikely to coincide unless the same mechanism governs the changes. Although previous studies explained this phenomenon by the wide and mixed distribution of the resistance and compliance vessel in the pulmonary vasculatures [24,30], our study found that the exact reciprocal changes in compliance and resistance might be associated with wall thickening and a reduced number of small arteries. Further studies are needed to clarify the contribution of proximal and peripheral arteries to compliance reduction.

In our study, SuHx-induced PH did not alter characteristic impedance. It remains unclear how PH impacts characteristic impedance [13–16], partly because its measurement in the frequency domain is imprecise. Characteristic impedance can be described by the inertia and compliance of proximal arteries as following [31]:

$$\text{Characteritic impedance} = \sqrt{\frac{\rho E h}{2\pi^2 r^5}}$$

where E, h, and r are the elastic module (Young's modulus), wall thickness, and luminal radius, respectively, of the proximal pulmonary artery, and ρ is the density of blood. Thus, it is conceivable that PH increases E and h and increases the radius of proximal arteries. Therefore, their net effect does not predict unidirectional changes in characteristic impedance.

4.3. Exploration of the clinical derivation of Z_{PA} in PH

Although we can obtain instantaneous pulmonary pressure and flow velocity instead of volumetric flow in clinical settings, irregular cardiac pacing, which is a prerequisite to derive precise estimations of the parameters in the 3-WK model, may be difficult to perform. To overcome this issue, we introduced parametric analysis of the 3-WK model under sinus rhythm in the time domain. We estimated pulmonary arterial pressure (P_{PA}) by convolving the impulse response of the 3-WK model with pulmonary arterial flow (F_{PA}) using the following equation:

$$P_{PA}(t) = \sum_{\tau=1}^{N} \frac{1}{C} \exp\left(-\frac{\tau}{RC}\right) F_{PA}(t-\tau) + Z_C F_{PA}(t) + P_D$$

where R, C, Z_C, and P_D are resistance, compliance, characteristic impedance, and downstream pressure, respectively, N is the total number of time series data ($N = 5000$), τ is the convolution parameter, and t is the time in increments of 1 ms. We determined resistance, compliance, and downstream pressure from the data of time series under sinus rhythm using the least-square method. The detailed derivation is provided in Supplement 3. Fig. 9A shows the estimated impedance obtained with this method superimposed on the impedance obtained with irregular pacing. We found that the time domain estimations of parameter values of resistance and compliance under sinus rhythm were as good as those obtained with irregular pacing in the frequency domain (Fig. 9B and C). Thus, it might be possible to assess Z_{PA} even in clinical settings.

4.4. Limitations

The present study has several limitations. First, we measured hemodynamics under general anesthesia. We used a mixture of α-chloralose and urethane. As both drugs are well known to affect hemodynamics by changing cardiac and vascular properties [32,33], we cannot directly extrapolate the results of this study to physiological hemodynamics under a conscious state. However, the trend in impedance associated with the progression of PH was preserved, because hemodynamics in all groups was assessed under the same condition. Second, the chest of the rats was open, and they were artificially ventilated with oxygen-enriched gas. These experimental conditions could have mechanically influenced the Z_{PA}. Furthermore, it is well known that the oxygen content in blood strongly alters PA characteristics and oxygen supplementation often reduces pulmonary artery pressure in PH patients [34]. However, oxygen supplementation was necessary for the stable measurement of hemodynamics, especially in the 8-week SuHx rats. Thus, we need to carefully interpret the impedance data in SuHx rats. Third, this study evaluated the histology associated with wall thickening in arteries with ODs < 50 μm and 50–100 μm. We could not evaluate larger pulmonary arteries with diameters > 100 μm, as most of these arteries were compressed by surrounding tissues and lost circularity. Further research is needed to clarify how these larger arteries affect pulmonary arterial resistance and compliance.

5. Conclusions

SuHx-induced PH markedly increased resistance and decreased compliance, while the time constant and characteristic impedance remained unaltered. These results indicate that resistant and compliant vessels are anatomically inseparable. We speculate that vascular remodeling in small arteries (ODs < 50 μm) is mostly responsible for these reciprocal changes in resistance and compliance. Our impedance analysis method might serve as a new tool to assess the progression of PH.

Supplementary data to this article can be found online at https://doi.org/10.1016/j.lfs.2018.10.005.

Acknowledgements

The authors thank Takuya Akashi, Takako Takehara and the staff of Center for Disruptive Cardiovascular Medicine, Kyushu University, Department of Cardiovascular Medicine, Kyushu University and Center for Clinical and Translational Research of Kyushu University Hospital for technical support.

Funding

This work was supported by Research and development of supportive device technology for medicine using Information and Communication Technology from Japan Agency for Medical Research and Development (18he1102003h0004), Development of Advanced Measurement and Analysis Systems from Japan Agency for Medical Research and Development (18hm0102041h0003), Mirai-iryou from Japan Agency for Medical Research and Development, Grant-in-Aid for Young Scientists (B) (18K15893) from the Japan Society for the Promotion of Science, and Actelion Academia Prize 2015.

Conflict of interest

Nishikawa T, Tohyama T, Abe K, Oga Y, Arimura T and Sakamoto T have nothing to declare. Saku K and Kishi T work in a department endowed by Omron Healthcare Co. Sunagawa K works in a department endowed by Omron Healthcare Co. and Actelion Pharmaceuticals Japan. Tsutsui H received honoraria from Daiichi Sankyo, Inc., Otsuka Pharmaceutical Co., Ltd., Takeda Pharmaceutical Company Limited, Mitsubishi Tanabe Pharma Corporation, Boehringer Ingelheim Japan, Inc., Novartis Pharma K.K., Bayer Yakuhin, Ltd., Bristol-Myers Squibb KK, and Astellas Pharma Inc., and research funding from Actelion Pharmaceuticals Japan, Daiichi Sankyo, Inc., and Astellas Pharma Inc.

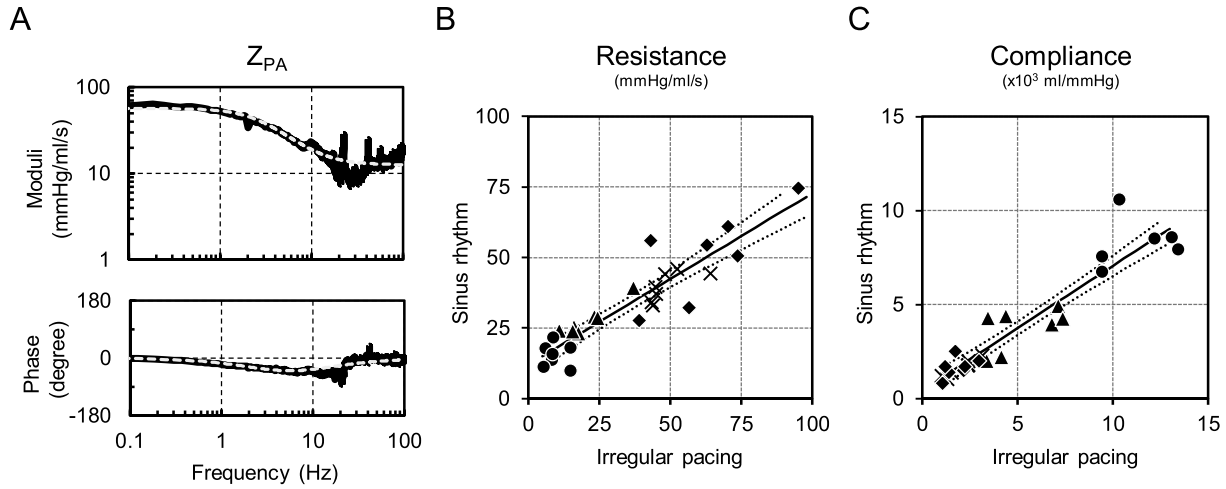

Fig. 9. Comparison of pulmonary arterial input impedance (Z_{PA}; solid line) and algebraically estimated impedance (dashed line) from the three-element windkessel (3-WK) parameters obtained from time series data under sinus rhythm. Estimated impedance accurately approximates Z_{PA} (A). Comparison of estimated resistance (B) and compliance (C) between irregular pacing and sinus rhythm. Parameters estimated under sinus rhythm match well with those estimated under irregular pacing. Each symbol indicates an individual rat. The circles, triangles, squares, and crosses represent baseline, SuHx1W, SuHx3W, and SuHx8W, respectively. The solid and dotted lines represent regression lines and their 95% confidence intervals, respectively. SuHx, Sugen/hypoxia.

References

[1] D.B. Badesch, G.E. Raskob, C.G. Elliott, A.M. Krichman, H.W. Farber, A.E. Frost, R.J. Barst, R.L. Benza, T.G. Liou, M. Turner, S. Giles, K. Feldkircher, D.P. Miller, M.D. McGoon, Pulmonary arterial hypertension: baseline characteristics from the REVEAL registry, Chest 137 (2010) 376–387, https://doi.org/10.1378/chest.09-1140.

[2] P. Escribano-Subias, I. Blanco, M. López-Meseguer, C.J. Lopez-Guarch, A. Roman, P. Morales, M.J. Castillo-Palma, J. Segovia, M.A. Gómez-Sanchez, J.A. Barbera, Survival in pulmonary hypertension in Spain: insights from the Spanish registry, Eur. Respir. J. 40 (2012) 596–603, https://doi.org/10.1183/09031936.00101211.

[3] H.I. Palevsky, B.L. Schloo, G.G. Pietra, K.T. Weber, J.S. Janicki, E. Rubin, A.P. Fishman, Primary pulmonary hypertension. Vascular structure, morphometry, and responsiveness to vasodilator agents, Circulation 80 (1989) 1207–1221.

[4] M.F. O'Rourke, M.G. Taylor, Input impedance of the systemic circulation, Circ. Res. 20 (1967) 365–380.

[5] M.G. Taylor, Use of random excitation and spectral analysis in the study of frequency-dependent parameters of the cardiovascular system, Circ. Res. 18 (1966) 585–595, https://doi.org/10.1161/01.RES.18.5.585.

[6] N. Westerhof, G. Elzinga, P. Sipkema, An artificial arterial system for pumping hearts, J. Appl. Physiol. 31 (1971) 776–781.

[7] W.R. Milnor, C.R. Conti, K.B. Lewis, M.F. O'Rourke, Pulmonary arterial pulse wave velocity and impedance in man, Circ. Res. 25 (1969) 637–649.

[8] R.L. Benza, D.P. Miller, M. Gomberg-Maitland, R.P. Frantz, A.J. Foreman, C.S. Coffey, A. Frost, R.J. Barst, D.B. Badesch, C.G. Elliott, T.G. Liou, M.D. McGoon, Predicting survival in pulmonary arterial hypertension: insights from the registry to evaluate early and long-term pulmonary arterial hypertension disease management (REVEAL), Circulation 122 (2010) 164–172, https://doi.org/10.1161/CIRCULATIONAHA.109.898122.

[9] I.T. Rosen, H.L. White, The relation of pulse pressure to stroke volume, Am. J. Phys. 78 (1927) 168–184.

[10] K. Sunagawa, W.L. Maughan, K. Sagawa, W. Lowell, Stroke volume effect of changing arterial input impedance over selected frequency ranges, Am. J. Phys. 248 (1985) H477–H484.

[11] J.P. Murgo, N. Westerhof, J.P. Giolma, S.A. Altobelli, Aortic input impedance in normal man: relationship to pressure wave forms, Circulation 62 (1980) 105–116, https://doi.org/10.1161/01.CIR.62.1.105.

[12] J.P. Murgo, N. Westerhof, Input impedance of the pulmonary arterial system in normal man. Effects of respiration and comparison to systemic impedance, Circ. Res. 54 (1984) 666–673, https://doi.org/10.1161/01.RES.54.6.666.

[13] W.K. Laskey, V.A. Ferrari, H.I. Palevsky, W.G. Kussmaul, Pulmonary artery hemodynamics in primary pulmonary hypertension, J. Am. Coll. Cardiol. 21 (1993) 406–412.

[14] M. Maggiorini, S. Brimioulle, D. De Canniere, M. Delcroix, R. Naeije, Effects of pulmonary embolism on pulmonary vascular impedance in dogs and minipigs, J. Appl. Physiol. 84 (1998) 815–821, https://doi.org/10.1152/jappl.1998.84.3.815.

[15] R.A. Hopkins, J.W. Hammon, P.A. Mchale, P.K. Smith, An analysis of the pulsatile hemodynamic responses of the pulmonary circulation to acute and chronic pulmonary venous hypertension in the awake dog, Circ. Res. 47 (1980) 902–910.

[16] D.H. Bergel, W.R. Milnor, Pulmonary vascular impedance in the dog, Circ. Res. 16 (1965) 401–415, https://doi.org/10.1161/01.RES.16.5.401.

[17] K. Abe, M. Toba, A. Alzoubi, M. Ito, K.A. Fagan, C.D. Cool, N.F. Voelkel, I.F. McMurtry, M. Oka, Formation of plexiform lesions in experimental severe pulmonary arterial hypertension, Circulation 121 (2010) 2747–2754, https://doi.org/10.1161/CIRCULATIONAHA.109.927681.

[18] C.L. Lucas, B.R. Wilcox, B. Ha, G.W. Henry, Comparison of time domain algorithms for estimating aortic characteristic impedance in humans, IEEE Trans. Biomed. Eng. 35 (1988) 62–68, https://doi.org/10.1109/10.1337.

[19] A.R. Conn, N.I.M. Gould, P.L. Toint, Trust Region Methods, Society for Industrial and Applied Mathematics, Philadelphia, 2000.

[20] R.T. Schermuly, E. Dony, H.A. Ghofrani, S. Pullamsetti, R. Savai, M. Roth, A. Sydykov, Y.J. Lai, N. Weissmann, W. Seeger, F. Grimminger, Reversal of experimental pulmonary hypertension by PDGF inhibition, J. Clin. Invest. 115 (2005) 2811–2821, https://doi.org/10.1172/JCI24838.

[21] R. Jones, W.M. Zapol, L. Reid, Pulmonary artery remodeling and pulmonary hypertension after exposure to hyperoxia for 7 days. A morphometric and hemodynamic study, Am. J. Pathol. 117 (1984) 273–285.

[22] S.R. Reuben, Compliance of the human pulmonary arterial system in disease, Circ. Res. 29 (1971) 40–50, https://doi.org/10.1161/01.RES.29.1.40.

[23] J.-W. Lankhaar, N. Westerhof, T.J.C. Faes, C.T.-J. Gan, K.M. Marques, A. Boonstra, F.G. van den Berg, P.E. Postmus, A. Vonk-Noordegraaf, Pulmonary vascular resistance and compliance stay inversely related during treatment of pulmonary hypertension, Eur. Heart J. 29 (2008) 1688–1695, https://doi.org/10.1093/eurheartj/ehn103.

[24] N. Saouti, N. Westerhof, F. Helderman, J.T. Marcus, N. Stergiopulos, B.E. Westerhof, A. Boonstra, P.E. Postmus, W. Be, P. Pe, A. Vonk-Noordegraaf, W. Be, P. Pe, RC time constant of single lung equals that of both lungs together: a study in chronic thromboembolic pulmonary hypertension, Am. J. Physiol. Heart Circ. Physiol. 297 (2009) H2154–H2160, https://doi.org/10.1152/ajpheart.00694.2009.

[25] J. Pfitzner, Poiseuille and his law, Anaesthesia 31 (1976) 273–275.

[26] A. Hislop, L. Reid, New findings in pulmonary arteries of rats with hypoxia-induced pulmonary hypertension, Br. J. Exp. Pathol. 57 (1976) 542–554.

[27] D. Ryland, L. Reid, The pulmonary circulation in cystic fibrosis, Thorax 30 (1975) 285–292, https://doi.org/10.1136/thx.30.3.285.

[28] R. Kobs, N. Muvarak, J. Eickhoff, N. Chesler, Linked mechanical and biological aspects of remodeling in mouse pulmonary arteries with hypoxia-induced hypertension, Am. J. Physiol. Heart Circ. Physiol. 288 (2005) 1209–1217.

[29] R.H. Cox, Pressure dependence of the mechanical properties of arteries in vivo, Am. J. Phys. 229 (1975) 1371–1375, https://doi.org/10.1152/ajplegacy.1975.229.5.1371.

[30] C.A. Dawson, D.A. Rickaby, J.H. Linehan, T.A. Bronikowski, Distributions of vascular volume and compliance in the lung, J. Appl. Physiol. 64 (1988) 266–273.

[31] Z. Wang, N.C. Chesler, Pulmonary vascular wall stiffness: an important contributor to the increased right ventricular afterload with pulmonary hypertension, Pulm. Circ. 1 (2011) 212–223, https://doi.org/10.4103/2045-8932.83453.

[32] D.M. Beam, E.M. Neto-Neves, W.B. Stubblefield, N.J. Alves, J.D. Tune, J.A. Kline, Comparison of isoflurane and α-chloralose in an anesthetized swine model of acute pulmonary embolism producing right ventricular dysfunction, Comp. Med. 65 (2015) 54–61.

[33] T.D. Giles, A.C. Quiroz, G.E. Burch, Hemodynamic alterations produced by prolonged urethane anesthesia in the intact dog, Am. Heart J. 78 (1969) 281–282, https://doi.org/10.1093/eurheartj/ehv764.

[34] S.H. Dressler, N.B. Slonim, O.J. Balchum, G.J. Bronfin, A. Ravin, The effect of breathing 100% oxygen on the pulmonary arterial pressure in patients with pulmonary tuberculosis and mitral stenosis, J. Clin. Invest. 31 (1952) 807–814, https://doi.org/10.1172/JCI102666.